Development and Characterization of a Hydrogel Containing Silver Sulfadiazine for Antimicrobial Topical Applications.
Part II: Stability, Cytotoxicity and Silver Release Patterns

Lilian Vieira Vaz[1], Victor Manuel Balcão[1,2],
José Martins Oliveira Jr.[1], Matthieu Tubino[3], Angela Jozala[1],
Valquíria Miwa Hanai Yoshida[1], Marta Maria Duarte Carvalho Vila[1]*

[1]PhageLab- Laboratory of Biofilms and Bacteriophages, University of Sorocaba Campus Cidade Universitária Prof. Aldo Vannucchi, Sorocaba/SP, Brazil, [2]Department of Biology and CESAM, University of Aveiro, Campus Universitário de Santiago, Aveiro, Portugal, [3]Institute of Chemistry, University of Campinas, Campinas/SP, Brazil

Hydrogels are interesting for use in the treatment of topical wounds due to their virtually zero toxicity, and capacity for extended release of pharmaceuticals. Silver sulfadiazine (SSDZ) is the drug of choice in the treatment of skin burns. The aim of the study was to determine cytotoxicity, antimicrobial activity and stability of a PVA hydrogel with integrated silver sulfadiazine. SSDZ-hydrogels were prepared using 10% (w/w) PVA (either 89% or 99% hydrolyzed) and 1% (w/w) silver sulfadiazine. Cellular viability was assessed via MTS assays, antimicrobial activity via disk-diffusion and accelerated stability tests were carried out with analysis at 0, 30, 60, 90 and 180 days of storage at 40 ± 2 °C and a relative humidity of 75 ± 5 %. The parameters evaluated included organoleptic characteristics, moisture, swelling ability, mechanical strength, FTIR, XRD, TGA and DSC, and silver release patterns via XRD and potentiometry. Cell viability tests indicated some cytotoxicity, although within acceptable levels. After 90 days of storage, SSDZ hydrogel samples exhibited a brown coloration, probably due to the formation of Ag or Ag_2O nanoparticles. The SSDZ-loaded hydrogels suffered visual and physical changes; however, these changes did not compromise its use as occlusive wound dressings or its antimicrobial properties.

Keywords: Hydrogel. Silver sulfadiazine. Antimicrobial topical applications.

INTRODUCTION

Biotechnology has contributed greatly to the development of numerous sectors, with health being one of the fields in which this technology has had the most impact. Hydrogels, also termed "smart and/or hungry networks", are currently the focus of considerable scientific research due to their potential for hi-tech applications in the biomedical, pharmaceutical, biotechnology,

bioseparation, biosensor, agriculture, oil recovery and cosmetic fields (Ullah *et al.*, 2015). To this end, many hydrogels are being developed as tissue-engineered scaffolds (Yu *et al.*, 2015); material for biosensors (Schmidt *et al.*, 2016); smart carriers for multiple cargos (Sepantafar *et al.*, 2017); wound dressing and among other applications (Chirani *et al.*, 2015). Hydrogels are dosage forms whose structure is characterized by a three-dimensional network of hydrophilic polymers which, upon contact with water, swell while maintaining their integrity (Ahmed, 2015). Hydrogels allow a marked decrease in the number of topical applications, better adherence of patients to treatment while also reducing adverse side

effects (Vashist *et al.*, 2014). Hence, hydrogels are highly attractive for the treatment of skin wounds due to their non-toxic in nature, capacity for the controlled/prolonged release of pharmaceuticals and potential ability to keep the wound moist (Song, Rane, Christman, 2012). Thus, given the advantages observed in hydrogels for the treatment of wounds, especially skin burns, many researchers have developed and characterized hydrogels with silver compounds (Farjado *et al.*, 2013; Serra *et al.*, 2015). Regarding pharmaceutical products indicated for use in the treatment of skin burn injuries, there is a consensus on the use of silver sulfadiazine (SSDZ) at 1% (w/w) (International Consensus, 2012; Farjado *et al.*, 2013; Serra *et al.*, 2015). The development of a pharmaceutical formulation should guarantee effectiveness, efficiency, and safety to the consumer. The quality of a pharmaceutical product can be gathered from stability studies, determining the length of time during which the pharmaceutical product can be considered stable (i.e., able to maintain constant the characteristics that have been designed and developed) (Bajaj, Singla, Sakhuja, 2012). The stability of pharmaceutical formulations can be altered by extrinsic and intrinsic factors, with serious consequences for the quality of pharmaceutical products. Intrinsic factors are related to the interaction between the components of the formulation, which can influence the stability of a drug, produce alterations in pH value, viscosity, organoleptic characteristics, phase separations, reduction in the content of active substance, among others. Extrinsic or environmental factors are related to those that cause degradation following exposure to high temperatures, light, oxygen, moisture, and microorganisms (Bhagyashree *et al.*, 2015; Bajaj, Singla, Sakhuja, 2012; Guo, Shalav, Smith, 2013). Although of the various hydrogel-based products on the market, the development or optimization of hydrogel dressings still represents a very active research field (Madaghiele *et al.*, 2014), in order to meet diverse needs such as large-scale production, cost reduction, etc. For the success of a product and its industrial production, it is also necessary to evaluate its lifetime of the product, in order to ensure its effectiveness and maintenance of its physical properties over time. Considering these facts, the main goal of the research effort herein was to evaluate a PVA hydrogel incorporating SSDZ in relation to its cytotoxicity, antimicrobial activity and stability during a storage timeframe of 180 days. Additionally, the SSDZ-loaded hydrogel formulation was characterized physicochemically, encompassing surface morphology via Field Emission Scanning Electron Microscopy (FESEM), thermal analyses by Differential Scanning Calorimetry (DSC), infrared spectrophotometry with Fourier transform (FTIR), and X-ray diffraction analyses (XRD).

EXPERIMENTAL PROCEDURES

Preparation of hydrogels

The SSDZ-loaded hydrogels were prepared according to Jodar *et al.* (2015).

The first step in the preparation of the hydrogel consisted of obtaining aqueous dispersions of 10% PVA (w/w) using PVA (89% hydrolyzed average MW 85,000-124,000) (PVA89) from Dinâmica Produtos Químicos Ltda (Diadema/SP, Brazil), PVA (98.99% hydrolyzed average MW11,000-31,000) (PVA99) purchased from Sigma-Aldrich (St. Louis MO, USA) and silver sulfadiazine solution at 10%, (w/v) using silver sulfadiazine from Valdequímica Produtos Químicos Ltda (São Paulo/SP, Brazil) (100.06% pure, considering 29.3% silver). 100 g of PVA89 or PVA99 were solubilized in 1000 mL of ultrapure water and the mixture kept under magnetic stirring (ca. 300 rpm) and heat (ca. 80 ± 5 °C) for approximately 2 h. Subsequently, the mixture was stirred for ca. 6 min. at 5200 rpm using an UltraTurrax homogenizer (model T25D from IKA Werke GmbH & Co. KG, Staufen, Germany). The mixture was then under mechanical stirring at 80 ± 5 °C for approximately 2 h. After this period, the dispersions were kept at rest until the temperature equilibration with room temperature ($\pm$ 25 °C). The silver sulfadiazine solution (10%, w/v) was prepared by dispersing 10 g of silver sulfadiazine in 100 mL of polyethylene glycol 400 (PEG 400) purchased from Dinâmica Produtos Químicos Ltda (Diadema/SP, Brazil) at room temperature ($\pm$ 25 °C) and subjecting the mixture to magnetic stirring for 30 min (ca. 300 rpm). For 100 mL of hydrogel, 10 mL of PVA dispersions

(PVA99 and PVA89) were mixed and heated to $80 \pm 5\ ^\circ\text{C}$ under magnetic stirring (ca. 300 rpm) for ca. 10 min. Subsequently, the silver sulfadiazine solution was incorporated (at different proportions) and the resulting dispersion was maintained under magnetic stirring for a further 30 min (ca. 300 rpm). Subsequently, 0.5 mL of glutaraldehyde solution at 25 % (v/v) from Dinâmica Produtos Químicos Ltda (Diadema/SP, Brazil) were added. The resulting dispersion was poured into plastic molds and dried at $60\ ^\circ\text{C}$ in a Fanem incubator (model 515 A, Karnataka, India). The SSDZ- loaded hydrogels were then washed with phosphate buffer pH 7.0 to eliminate virtually all unreacted (free) glutaraldehyde molecules. The SSDZ-loaded hydrogels were packaged using laminated sachets for pharmaceutical use from Tepron Equipment Laboratories (São Paulo/SP, Brazil). For the cellular viability assays, several SSDZ-loaded hydrogels were prepared containing different concentrations of silver sulfadiazine, viz. 0, 1.0, 2.5, 5.0 and 10.0% (w/w), to check for possible cellular toxicity with increasing silver content.

Cytotoxicity potential of the SSDZ-loaded hydrogels, via the MTS assay

The L929 fibroblast cell line from Sigma-Aldrich (São Paulo/SP, Brazil) was cultured in Dulbecco's Modified Eagle's Medium (DMEM), pH 7.4, supplemented with fetal bovine serum (10% w/w) and antibiotics (100 IU mL^{-1} penicillin/100 uL mL^{-1} streptomycin sulfate) (1%, w/w). The cells were incubated at $37\ ^\circ\text{C}$ under a 5% CO_2 atmosphere for 48 h. The culture medium was removed, and cells washed with phosphate buffer solution free of calcium and magnesium (PBS-CMF). 1 mL of trypsin-EDTA solution (0.25%, w/v) (Sigma-Aldrich, São Paulo SP, Brazil) was added and allowed to act for 3 to 5 min to dissociate adherent cells from the bottom of the vessel. After trypsinization, the cells were washed with PBS-CMF, centrifuged at 300 rpm, resuspended in DMEM and counted in a Neubauer chamber. Approximately 3×10^4 cell/well were poured into each of the wells of a 24-well plate. To each well, 150 µL of DMEM was added with disk-shaped (7.0 mm in diameter) samples of the different SSDZ-loaded hydrogels. The 24-well plates were then incubated at $37\ ^\circ\text{C}$ under a 5% CO_2 atmosphere. Cellular viability was assessed at 24, 48 and 72 h. The controls used were PBS-CMF, DMEM, and hydrogen peroxide. After 2 h incubation of the cells with the MTS (3-(4,5-dimethylthiazol-2-yl)-5-(3-carboxymethoxyphenyl)-2-(4-sulfophenyl)-2H-tetrazolium, inner salt) from Sigma-Aldrich (St. Louis MO, USA), absorbances were measured at 490 nm in a microplate ELISA reader (Tecan model Infinite M200 Pro, with software Magellan, Männedorf, Switzerland) (Giannelli *et al.,* 2008).

Antimicrobial activity of the SSDZ-loaded hydrogels via disk diffusion method

The antimicrobial activity of the SSDZ-loaded hydrogels was determined by the disk diffusion method (CLSI, 2011). The assays were performed in triplicate using *Staphylococcus aureus* ATCC 10390 and *Pseudomonas aeruginosa* ATCC 9721 supplied by the Fundação Oswaldo Cruz (Fiocruz, Rio de Janeiro/RJ, Brazil). The bacterial strains were inoculated in TSB nutritive broth (Tryptone Soy Broth, HiMedia Laboratories, Mumbai, India) and kept at $37\pm0.5\ ^\circ\text{C}$. After 24 h, the cultures were inoculated on Petri plates with TSB (0.8%, w/v bacteriological agar, Prodimol Biotecnologia S.A., São Paulo/SP, Brazil) and the samples were applied on the inoculated medium. The samples were SSDZ-loaded hydrogel disks (diameter 7.0 mm; weight 8 ± 0.01 mg), negative control (PVA hydrogel disc without SSDZ, diameter 7.0 mm), and positive control (SSDZ diluted in PEG 400, 1% w/w). This solution was adsorbed onto a paper disk with diameter of 7.0 mm. The Petri plates were incubated under aerobic conditions at $37 \pm 0.5\ ^\circ\text{C}$. After 24 h, the plates were visually inspected for observation of growth inhibition halos.

Stability studies

Stability studies were performed during a timeframe of six months, with analyses at times 0 (24 h), 30, 60, 90 and 180 days (Bhagyashree *et al.*, 2015). The SSDZ-loaded hydrogel samples were kept in an incubator set at $40 \pm 2\ ^\circ\text{C}$ with 75 ± 5 % relative humidity (RH). The

parameters analyzed were morphological characteristics, moisture content, degree of swelling, antimicrobial activity via the disk diffusion method, mechanical resistance properties, FTIR, XRD, DSC, and silver release pattern via silver content determination by potentiometry.

Morphological characteristics

The SSDZ -loaded hydrogels were visually inspected considering color, odor, homogeneity, and presence or absence of cracks.

Moisture content analyses via infrared heating

Moisture determination of the SSDZ-loaded hydrogels was performed using a moisture analyzer equipped with a halogen lamp (Shimadzu, model MOC63U, Kyoto, Japan), with temperature ranging from 50 to 200°C. The parameters utilized for the analyses were 60°C in slow-heating mode.

Degree of swelling

The degree of swelling of the SSDZ-loaded hydrogels was determined according to the Enslin-Neff water adsorption test (Petkovsek, Macek, Majes, 2009) using Equation (1). All SSDZ-loaded hydrogel samples were submerged in 50 mL ultrapure water for 1, 3, 6, 12, 24 and 48 h. All swelling assays were performed in triplicate.

$$Swelling\ degree\ (\%) = \frac{p}{m_0} \times 100 = \frac{V \times d}{m_0} \times 100 \qquad (1)$$

where: $P = m_t - m_0$ is the mass of adsorbed water (g), m_t is the weight of (swelled) sample at time t (g), m_0 is the initial weight of dry sample (g); $V =$ is the volume of adsorbed water (mL); and $d =$ is the density of water (g.cm^{-3}) (Kiviranta, Kumpulainen, 2011).

Mechanical resistance properties

Properties including resistance to perforation, relaxation, and resilience were evaluated using a Texture Analyser from Stable MicroSystems (model TA.XT Plus, Godalming, United Kingdom). For determination

parameters, a distance of 5 mm was set for the perforation resistance tests, a distance of 2 mm for both resilience and relaxation tests, and a maximum force of 5 kg for all tests. All determinations were carried out in triplicate.

Fourier Transform Infrared Spectrophotometry (FTIR) analyses

The infrared spectra of SSDZ and SSDZ -loaded hydrogel samples were gathered using an FTIR spectrophotometer from Agilent (model Cary 630, Santa Clara CA, U.S.A.), in the wavenumber range from 4000 cm^{-1} to 400 cm^{-1}, with a resolution of 4 cm^{-1}, using Happ-Genzel apodization.

X-ray diffraction (XRD) analyses

X-ray diffractograms of SSDZ and SSDZ-loaded hydrogel samples were gathered on an X-ray Diffractometer (Shimadzu - model XRD7000, Kyoto, Japan), using X-ray radiation from a copper lamp with radiation Kα (λ = 1.5418 Å) filtered through a Cu target. The X-ray scanning was performed at diffraction angles of 2-Theta (from 5º to 90º, with increments of 0.02 degrees and rate of 2°min^{-1}), with a voltage of 40 kV, the electric current intensity of 30 mA, and X-ray power of 3 kW.

Thermal analyses via differential scanning calorimetry (DSC)

DSC analyses were performed using a differential scanning microcalorimeter from TA Instruments (model MDSC 2910, New Castle, U.S.A.). The samples were then heated from ca. 20 to 250 ºC, at a constant heating rate of 10 ºC min^{-1}, under a constant flow of argon of 50 mL min^{-1}. The data were gathered at a sampling rate of 0.2 seconds per data point.

Silver content determination by potentiometry for evaluation of silver release pattern

These assays were conducted using a silver chloride electrode coupled with a pH-meter Analyzer (model 300, as indicated in Jodar *et al.* (2015)). For these assays, ca. 0.100

g of SSDZ-loaded hydrogel samples were submerged in 20 mL of deionized water at a temperature of ca. 25±0.1 °C. A peristaltic pump (Ismatec, model MP13GJ-4, Glattbrugg, Switzerland) connected to Tygon tubing (2.54 mm φ_{int}), was used for the continuous removal and replacement of the reaction medium, at a flow rate of 0.5 mL min^{-1}. The DV (mV) of the aqueous medium in which the SSDZ-loaded hydrogels were immersed was gathered at pre-determined time intervals, using a silver electrode connected to a millivoltmeter. All measurements were gathered in mV/t$_{immersion of SSDZ-loaded hydrogel}$. The experiments were terminated when an SSDZ concentration plateau was reached.

Field Emission Scanning Electron Microscopy analyses (FESEM)

The surface and morphology of the cryogenic fracture of the SSDZ-loaded hydrogels were observed under a field emission scanning electron microscope (FESEM) (model QUANTA FEG 250, FEI Company, Hillsboro, U.S.A.) equipped with a field emission microscopy source. SSDZ-loaded hydrogel samples were plunged into liquid nitrogen with the aid of tweezers and, after 5 min of immersion, the deep-frozen SSDZ-loaded hydrogel samples were cracked. The cryogenically fractured samples were then sputter-coated with Au/Pd film (80%/20%) via cathodic pulverization on a carbon layer produced by evaporation in a metalizing device from *BAL-TEC* (model *BAL-TEC MED 020, BAL-TEC*, Balzers, Liechtenstein). Microphotographs were taken using electron beams with 10 keV energy.

Mathematical modeling of SSDZ release pattern from the hydrogel

The mathematical models were of the first order (equation 2), Higuchi (equation 3) and Korsmeyer-Peppas (equation 4).

$$LnQ_t = LnQ_0 + k_1 \times t \qquad (2)$$

where: Q_t = amount of drug released at time t; Q_0 = initial amount of drug in a dosage form; k_1 = release rate constant; t = time.

$$Q_t = k_H \cdot \sqrt{t} \qquad (3)$$

where: Q_t = amount of drug released at time t; k_H = Higuchi constant; t = time.

$$Q_t/Q_\infty = k_{KP} \cdot t^n \qquad (4)$$

where: Q_t = amount of drug released at time t; Q_∞ = total amount of drug dissolved when the dosage form (hydrogel) is exhausted; k_{KP} = Korsmeyer-Peppas kinetic constant; n = diffusion or release exponent; t = time.
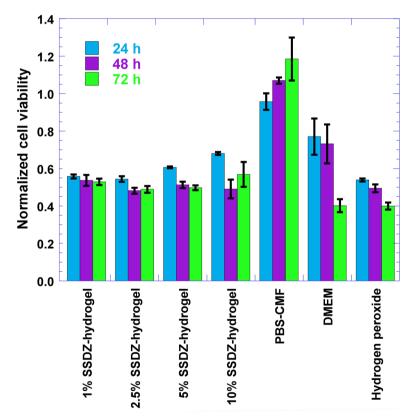
RESULTS AND DISCUSSION

Dressings that incorporate silver are a new modality for treatment of burns with multiple functions, acting both on bacterial control and on devitalized tissue removal, re-epithelization and pain control. There is a large variety of silver-based dressings available nowadays and their features were described in recent papers. Some examples are: Acticoat®; Acticoat Flex®, Mepilex Ag®; Aquacel Ag®; Biatain AG®, among others (Moser, Pereima, Pereima, 2013; Munteanu, Florescu, Niteseu, 2016; Hora *et al.*, 2017). The film developed in this work presented similar properties to the products already available in the market. However, due to the simplicity of its components, the cost of production may be lower, hence being accessible to a larger number of people. The SSDZ-loaded hydrogel with 1% (w/w) of SSDZ was chosen as the most adequate. This concentration is typically used in the treatment of burns and is likely to promote fewer toxicity problems. According to Lansdown (2010), clinical trials with silver dressings have shown that most of the silver ions released into the wound are deposited superficially and that the levels available for absorption are minimal. The absorption of silver by intact skin is low (<1 ppm), since most free ions are precipitated in the form of silver sulphide (Ag$_2$S) in the outer part of the stratum corneum. In injured skin, silver absorption of up to 10% can occur when used on burns located in highly vascularized regions (Lansdown, 2006). In addition, if systemically absorbed, silver is excreted mainly in the faeces and urine and

is not absorbed into the central or peripheral nervous system (International Consensus, 2012). Allergy is one of the few known contraindications for the topical use of silver (Lansdown, 2006). However, hepatic toxicity, renal toxicity, and leukopenia have been reported in large wound treatments using topical application of silver sulfadiazine, but with use justified by their antimicrobial efficacy (Shahzad, Ahmed, 2013). PVA was utilized for the preparation of the SSDZ-loaded hydrogels because it displays good plasticity characteristics for producing films and is a non-toxic biocompatible polymer with appropriate thermal, chemical and mechanical resistances (Baker *et al.,* 2012; Murphy *et al.*, 2012; Vila *et al.*, 2014). The SSDZ-loaded hydrogels developed have PVA in

their composition, a relatively hydrophobic polymer with a low surface free energy (Asadinezhad *et al.*, 2012) that does not favor attraction of water molecules from the dispersion containing the polymers, most likely due to the hydrophobic effect (decrease in interfacial free energy). Consequently, this promotes the non-adherence of the hydrogel to the bandages and dressings that may be utilized to keep it in place.

Cell viability assays

Figure 1 depicts the mitochondrial activity produced by the SSDZ-loaded hydrogels during three cell contact periods (viz. 24, 48 and 72 h).

FIGURE 1 - Normalized cell viability (via MTS assays) to evaluate the cytotoxicity of SSDZ-free hydrogel and SSDZ-loaded hydrogels containing different concentrations of silver sulfadiazine (n=3).

Silver dressing cytotoxicity is an inevitable consequence of the silver antimicrobial activity as report by other authors (Boutrand, 2012; Hiro *et al.*, 2012). In

this sense, silver-based dressing products, as well as antimicrobial dressings, are recommended only for: contaminated burns; clinically infected burns; deep or

full thickness burns; burns of mixed or unknown depth and minor burns with larger surface areas (Muntaenu *et al.*, 2016). The objective of cytotoxicity testing by the MTT method was to determine which concentration was the most adequate for the development of the hydrogel and if higher silver concentrations would significantly increase the hydrogel toxicity. The results show that all the hydrogels, including the one with 10% (w/w) SSDZ, presented, after 48 h of contact, results in cellular viability between 50% and 70%. According to the ISO 10993 (ISO, 2009), reduction of cell viability higher than 30% is considered a cytotoxic effect (Boutrand, 2012). It can be observed that an increase occurred in cell viability in the hydrogels with a higher content of SSDZ for 24 h. Within the limitations of this *in vitro* study, one can intuit that hydrogels with a higher content of SSDZ tend to be more cytotoxic over time because of the prolonged release of silver. With high concentrations of Ag high oxidative stress occurs by decreasing glutathione (GSH) and superoxide dismutase (SOD) and increasing lipid peroxidation, which finally leads to apoptosis by increasing caspase-3 activity and DNA fragmentation (Zhang *et al.*, 2014).

Thus, it can be stated that the hydrogels obtained cannot be considered cytotoxic. The cell viability and mitochondrial activity after 72 h of contact with SSDZ-loaded hydrogels were higher than those observed by Rigo *et al.* (2013) that, when testing silver nanoparticles, observed cell viability of only 17% after 72 h of contact with the particles. Conversely, the substance used as the positive control (hydrogen peroxide) promoted the highest levels of cell death (i.e., the lowest cell viability), as expected. The DMEM medium also promoted a marked decrease in cell viability when compared with the buffer system utilized. Upon addition of PBS buffer, Ag^+ likely reacts with Cl^- to produce AgCl, thereby decreasing the bioavailability of Ag^+ and cytotoxicity of Ag^+. The silver ions with SO_4^{2-}, S^{2-}, Cl^-, PO_4^{3-}, and EDTA can form ligations and reduce silver toxicity by the formation of Ag_xS_y (McShan, Ray, Yu, 2014).
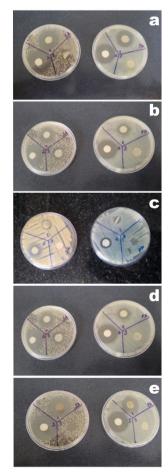
Antimicrobial properties

Table I and Figure 2 show the antimicrobial efficiency of the SSDZ-loaded hydrogels throughout the storage timeframe. The assays were carried out in duplicate, using a strain of *Staphylococcus aureus* ATCC 10390 and a strain of *Pseudomonas aeruginosa* ATCC 9721 because these are the most commonly isolated bacteria from chronic wounds (Serra *et al.*, 2015). The disk diffusion test is a simple and practical method which uses antimicrobial substances impregnated in wafers (disk) to test whether a particular bacteria is susceptible to a specific antibiotic or otherwise. The term "susceptible" represent that isolates are inhibited by the usually recommended dosage of an antimicrobial agent. However, there may be imprecision in the result. This imprecision is due to the effect of host responses, site of infection, toxin production by bacteria that is independent of antimicrobial susceptibility, the presence of biofilm, drug pharmacodynamics and other factors (Bagul, Sivakumar, 2016). In this research, the disk diffusion test was used because the objective was only to monitor the antimicrobial activity of the hydrogel over time.

The data obtained from the antimicrobial activity evaluation were submitted to the ANOVA test using a level of significance (α) of 0.05. In order to decide between the hypotheses H0 (*there is no difference between average inhibition halos at different storage times*) and H1 (*at least two average inhibition halos at different storage times differ from one another*). If *F-calculate> F-tabulated*, we reject H0, else if *F-calculate (F_{cal}) ≤ F-tabulated (F-tab)*, we do not reject H0. For *Pseudomonas aeruginosa* F_{cal} = *0.79727* and *F-$_{tab}$= 3.11* for df = *4* (degrees of freedom). For *Staphylococcus aureus* F_{cal} = 0.756504 and F-tab= 3.11 for df = 4 (degrees of freedom). In these cases, there is no evidence of differences between average inhibition halos at different storage times for the two microorganisms studied (*Staphylococcus aureus* and *Pseudomonas aeruginosa).*

Lilian V. Vaz, Victor M. Balcão, José M. Oliveira Jr., Matthieu Tubino, Angela Jozala, Valquíria M. H. Yoshida, Marta M. D. C. Vila

TABLE I - Growth inhibition halos produced by the SSDZ-hydrogel throughout storage time (0, 30, 60, 90 and 180 d). Positive control: SSDZ at 1% (w/w); Negative control: SSDZ-free hydrogel; n=3.
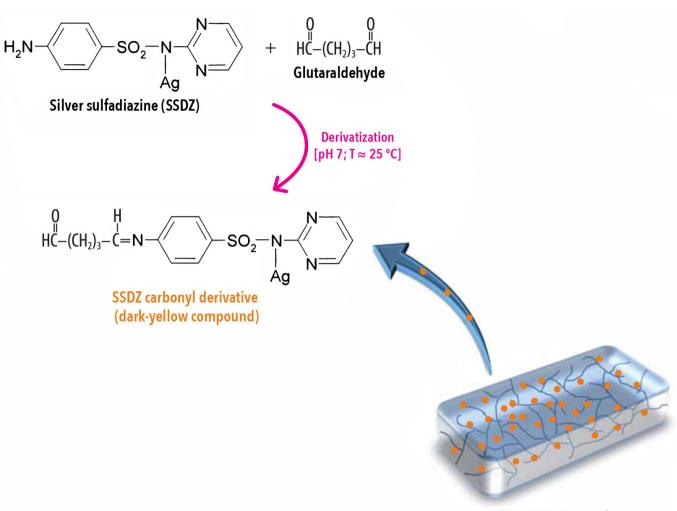
Storage time (d)	Inhibition halos Staphylococcus aureus (mm)	Inhibition halos Pseudomonas aeruginosa (mm)	%Inhibition degree Staphylococcus aureus	%Inhibition degree Pseudomonas aeruginosa
0	224 ± 6	251 ± 7	114.09	86.55
30	210 ± 7	238 ± 5	108.18	82.07
60	197 ± 6	217 ± 7	89.54	74.83
90	187 ± 4	202 ± 6	85.00	69.65
180	186 ± 6	197 ± 5	84.54	67.93
Positive control	220 ± 5	290 ± 7	100.00	100.00
Negative control	0.00	0.00	0.00	0.00

FIGURE 2 - Antimicrobial activity by disc-diffusion assay for *Pseudomonas aeruginosa* and *Staphylococcus aureus*. 1: SSDZ-loaded hydrogel samples at 0d (a), 30d (b), 60d (c), 90d (d) and 180d (e); 2: positive inhibition control (SSDZ aqueous solution at 1% (w/v)); 3: negative inhibition control (SSDZ-free hydrogel).

Coloration

During the stability assays, the SSDZ-loaded hydrogel samples exhibited darkening after 60 days of storage. The dark brown color might be due to the formation of Ag or Ag_2O nanoparticles. Darkening of synthesized silver nanoparticles is expected and can be used to monitor the formation and stability of silver nanoparticles (Meva *et al.*, 2016). Other authors suggest that the aldehyde groups from residual (free) glutaraldehyde molecules following reticulation of the polymeric hydrogel might react with amine groups from incorporated SSDZ, promoting a derivatization reaction with concomitant production of an SSDZ carbonyl derivative and darkening of the SSDZ-loaded hydrogels, a color change consistent with results published elsewhere (Balcão *et al.*, 2001a; 2001b; Lamas *et al.,* 2001). The probable reaction is shown in Figure 3. The results of the stability assays indicate that the hydrogels should be kept at refrigerated temperature (2 ° to 8 ° C) in order to avoid or minimize darkening.

FIGURE 3 - Mechanism of reaction between silver sulfadiazine (SSDZ) and glutaraldehyde (GA).

Moisture

The average moisture content of the SSDZ-loaded hydrogels, collected throughout the storage timeframe, was 7.684±0.478 % (see Table II).

TABLE II - Moisture content of the SSDZ hydrogel produced and stored under specific conditions ((25±2) °C and (60±5)% RH), throughout storage time.

Storage time (d)	Moisture content (%, w/w)
0	8.45 ± 1.38
30	7.92 ± 2.04
60	7.62 ± 2.67

(continues on the next column...)

Storage time (d)	Moisture content (%, w/w)
90	7.45 ± 1.53
180	6.98 ± 2.94

The humidity data obtained were submitted to ANOVA testing adopting a level of significance (α) of 0.05. In order to decide between the hypotheses H0 (*there is no difference between average humidity values at different storage times*) and H1 (*at least two average humidity values at different storage times differ from one another*). If *F-calculate> F-tabulated*, we reject H0, else if *F-calculate (F_{cal}) ≤ F-tabulated (F-tab)*, we do not reject H0. The value of $F_{cal}= 0.185631$ *and* $F_{tab}= 3.11$ for df = 4 (degrees of freedom). In this case, there

was no evidence of differences between mean humidity values. The relatively low moisture content in the SSDZ-loaded hydrogels reduces the possibility of degradation by hydrolysis and proliferation of contaminating microorganisms.

Swelling degree

Figure 4 depicts the swelling ability of SSDZ-loaded hydrogels. The results obtained reveal no significant changes in the liquid absorption capability of the SSDZ-loaded hydrogels throughout storage time. However, the swelling degree of the hydrogels loading SSDZ after 90 days storage was the lowest. Maximum swelling occurred by the end of the first twelve hours of contact with the solvent. After this time period, the hydrogel samples stored for different periods of time absorbed a smaller amount of water, probably due to saturation of the films. Osmotic pressure forces, electrostatic forces, and viscoelastic restoring forces are the three main forces governing the swelling behavior of hydrogels (Ganji, Vasheghani-Farahani,Vasheghani-Farahani, 2010). In this way, the swelling behavior as well as kinetics and thermodynamic of swelling of hydrogels are very complex and influenced by several factors. Maybe continuous reactions happen between glutaraldehyde and SSDZ since the glutaraldehyde exhibit the ability to react and crosslink with proteins and amino groups, leading to the formation of a broad range of conjugates (Migneault *et al.*, 2004) affecting the swelling degree of the hydrogels during storage time.
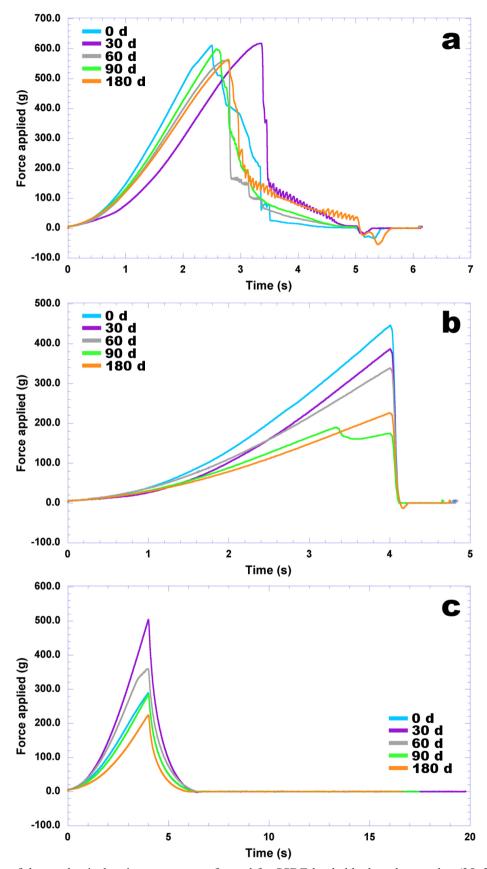

FIGURE 4 - Water adsorption assays of SSDZ-loaded hydrogels stored for different periods of time at (25±2) °C and (60±5)% RH, demonstrating the swelling ability of the SSDZ-loaded hydrogels.

Mechanical resistance

The results of the mechanical resistance (perforation, relaxation, and resilience) are depicted in Figure 5. The mechanical properties of the SSDZ-loaded hydrogels are mainly related to the polymer's ability to form bonds in polymer chains, impeding their separation when subject to mechanical forces (Yang, 2012).
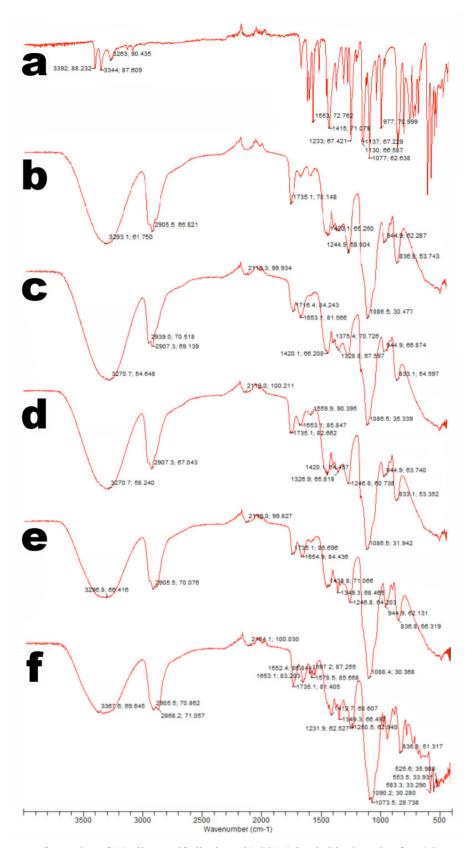
FIGURE 5 - Results of the mechanical resistance tests performed for SSDZ-loaded hydrogels stored at (25±2) °C and (60±5)% RH, for different storage times. (a) resistance to perforation, (b) relaxation, (c) resilience.

The SSDZ-loaded hydrogel exhibited a higher resistance after 30 days of storage than initially. The resistance to perforation (Figure 5a) gradually decreased over storage time after the first 30 days of storage, while maintaining intensity, which remained similar to that of the recently prepared SSDZ-loaded hydrogels. Comparison of relaxation throughout the storage timeframe reveals that the relaxation characteristics were maintained but consistently decreased in intensity throughout the storage timeframe (Figure 5b). Regarding the resilience features of the SSDZ-loaded hydrogels (Figure 5c), the same trend was observed as for perforation, in that the SSDZ-loaded hydrogels displayed a marked increase in resilience after the first 30 days of storage but consistently decreased in resilience thereafter. Hence, it may be concluded that the viscoelastic characteristics of deformation and molecular relaxation were improved during the first 30 days of storage and showed a consistent (albeit slight) decrease over the rest of the storage timeframe.

Fourier Transform Infrared (FTIR) analyses

Comparing the spectrum of silver sulfadiazine (Figure 6a) with that of the SSDZ-loaded hydrogels produced (Figure 6b), it can be observed that the characteristic peaks of silver sulfadiazine in the region from 1300 cm^{-1} to 1100 cm^{-1} are present in the SSDZ-loaded hydrogels (Figure 6b), but with a reduction in peak intensity. This suggests that the chemical aspect of SSDZ was preserved during the production of the SSDZ-loaded hydrogels. SSDZ did not engage in any chemical interactions with the hydrogel components and was only carried by the hydrogel. The FTIR spectra of the SSDZ-loaded hydrogels remained almost constant throughout the entire storage timeframe, further supporting that no significant chemical interactions occurred between the SSDZ-loaded hydrogel components.

FIGURE 6 - FTIR spectra of samples of (a) silver sulfadiazine, (b) SSDZ-loaded hydrogels after 0d storage, (c) SSDZ-loaded hydrogels after 30d storage, (d) SSDZ-loaded hydrogels after 60 d storage, (e) SSDZ-loaded hydrogels after 90 d storage, (f) SSDZ-loaded hydrogels after 180 d storage.
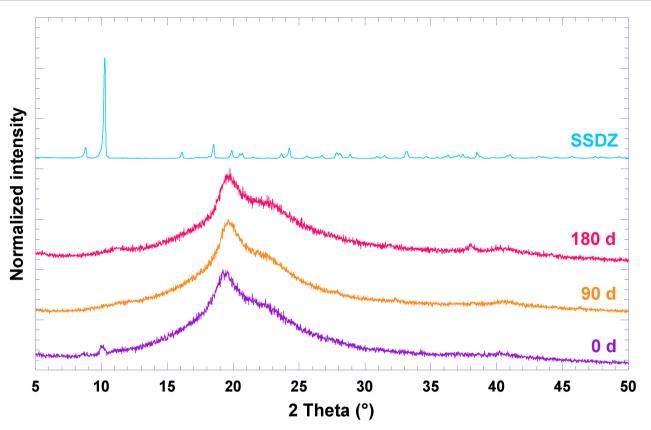
PVA reacted with glutaraldehyde via hydrogen bonding, which can be observed in stretching vibrations between 3330-3350 cm^{-1} (Reis *et al.*, 2006). In this wavenumber region, the large peak observed is most likely accounted for by hydroxyl groups from water molecules. Peaks near 3290 cm^{-1} are probably attributable to the crosslinking reaction. According to Matty, Sultan and Amine (2015), the peaks around 3386-3392 cm^{-1} indicate crosslinking to PVA with glutaraldehyde and acetal formation. Furthermore, according to Reis *et al.* (2006), the presence of peaks near 1720 cm^{-1} is probably the result of free aldehyde groups from glutaraldehyde, i.e., aldehyde groups that did not react with OH groups from the PVA chain. As glutaraldehyde is a bifunctional crosslinking agent, one aldehyde group would react with the polymer chain of PVA forming a hemiacetal structure, while the other would remain unreacted as a function of a conformational or kinetic limitation (Sadahira, Souza, Mansur 2007). The amine group from SSDZ is accounted for by peaks between 2950-3000 cm.$^{-1}$ These peaks are evident in all spectra (Figures 5b-f), with decreasing intensities throughout the storage timeframe. Characteristic peaks indicative of SSDZ lie between 1390 cm^{-1} and 1250 cm^{-1} for C-N bonds, between 1640 cm^{-1} and 1500 cm^{-1} for N-H groupings, close to 1050 cm^{-1} corresponding to the S=O$_2$ bond, between 3500 cm^{-1} and 3300 cm^{-1} corresponding to OH groups, and between 2950 cm^{-1} and 3000 cm^{-1} representing C-H bonds (Mehta *et al.*, 2013).

X-ray diffraction (XRD) analyses

The results of the X-ray diffraction analyses (XRD) performed for the SSDZ-loaded hydrogels are depicted in Figure 7 in the form of normalized diffractograms and reveal amorphous behavior without peaks of crystallinity. The small peaks at 2θ $\rho \cong$ 41° in the diffractograms of SSDZ-loaded hydrogels at times 0, 90, and 180 days are most likely related to the presence of residual water in the SSDZ-loaded hydrogel samples.
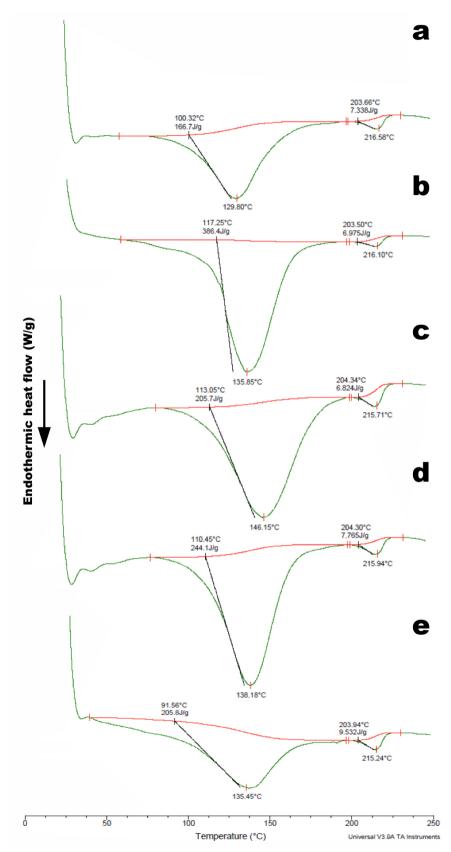
The diffractograms of SSDZ and of the SSDZ-loaded hydrogels at time 0 d display a characteristic peak attributed to SSDZ at 2θ $\cong$ 10°. This peak is absent from the diffractogram of SSDZ-loaded hydrogels at 90 and at 180 days of storage and is congruent with the probable reaction between the aldehyde group in residual (free) glutaraldehyde molecules and the amine group of SSDZ, that most likely caused the darkening of the SSDZ-loaded hydrogels during storage. On the other hand, the dark brown color might be due to the formation of Ag or Ag$_2$O nanoparticles (Eya'ane Meva *et al.*, 2016). Figure 7 (180 d) shows a weak diffraction peak at 2θ ~ 38 ° that can be ascribed to the reflection of planes of the face-centered cubic Ag or planes of Ag$_2$O nanocrystals. Normalization of diffractograms was performed by dividing the intensity values by the maximum intensity value in each diffractogram, allowing a better comparison between the X-ray diffractograms of the SSDZ-loaded hydrogels. The X-ray diffractogram patterns for the SSDZ-loaded hydrogels have the same intensity pattern throughout storage time, but with different amplitudes for some peaks, indicating that there were no significant changes in the structure of the hydrogel. The X-ray diffractogram patterns displayed characteristic peaks of crystallinity at 2θ $\cong$ 19° (higher intensity), 2θ $\cong$ 22° (less defined and shallow) and a wide range of low intensity signals, indicating the dominance of amorphous structure in the hydrogel. The results obtained were very similar to those reported by Parparita *et al.* (2014), showing that PVA produces crystallinity peaks at 2θ $\cong$ 19.59° and 2θ $\cong$ 22°.

FIGURE 7 - Normalized X-ray diffractograms (XRD) of samples of silver sulfadiazine (SSDZ) and of samples of SSDZ-loaded hydrogels (0d), SSDZ-loaded hydrogels after 90 d storage, and SSDZ-loaded hydrogels after 180 d storage.

Thermal analyses by differential scanning calorimetry (DSC)

The DSC thermograms of the SSDZ-loaded hydrogels samples exhibit two major endothermal events (Figure 8 and Table III).

FIGURE 8 - Differential scanning calorimetry thermograms of samples of recently prepared SSDZ-loaded hydrogels (a), SSDZ-loaded hydrogels after 30 d storage (b), SSDZ-loaded hydrogels after 60 d storage (c), SSDZ-loaded hydrogels after 90 d storage (d), and SSDZ-loaded hydrogels after 180 d storage (e).

TABLE III - Thermal events in the DSC analyses of SSDZ hydrogel produced and stored under specific conditions ((25±2) °C and (60±5)% RH), throughout storage time.

Storage Time (d)	1st Endothermal event		2nd Endothermal event		Melting range DT (°C)
	Peak temperature (°C)	Melting enthalpy (J/ gSSDZ-hydrogel)	Peak temperature (°C)	Melting enthalpy (J/ gSSDZ-hydrogel)	
0	129.80	166.7	216.58	7.338	86.78
30	135.85	386.4	216.10	6.975	80.25
60	146.15	205.7	215.71	6.824	69.56
90	138.18	244.1	215.94	7.765	77.76
180	135.45	205.8	215.24	9.532	79.79

Peppas and Merrill (1976) studied PVA-based hydrogels and observed melting point temperatures ranging from ca. 208.2 °C to 216.5 °C, depending on the amount of PVA in the hydrogel and the type of crosslinking. The results obtained in the DSC analyses of SSDZ-loaded hydrogels show maintenance of the peak temperature of the second endothermal event. Regarding the first endothermal event, its peak temperature was displaced only slightly back and forth, which is an indication that no significant changes occurred throughout storage time in the structure of the SSDZ-loaded hydrogels, such as polymerizations, oxidations, desorption, among other phenomena. However, the melting enthalpy of the first endothermal event at 30 d of storage reveals an increase in the melting enthalpy of ca. 132% followed by a decrease of ca. 47% at 60 d of storage, with subsequent increase and decrease in the order of ca. 20% at 90 d and 180 d of storage, respectively. These changes in melting enthalpies are likely attributable to the derivatization reaction between glutaraldehyde and SSDZ. The melting range, however, remained almost constant throughout the storage timeframe. Differential scanning calorimetric analyses of the SSDZ-loaded hydrogel formulation provided an insight into the state and degree of crystallinity, and the melting and crystallization behavior of crystalline materials. The second endothermal event, occurring at around 216 °C, was most likely related to decomposition events. The results of the DSC thermal analyses of the SSDZ-loaded hydrogels are in close agreement with those obtained from X-ray diffraction studies (Figure 7). Examination of the DSC thermograms shows that impregnation of the hydrogel with SSDZ led to decreased crystallinity and narrowing of the melting profile. Notably, the thermal events depicted in Figure 8 and the X-ray diffractograms depicted in Figure 7 denote amorphization of the SSDZ-loaded hydrogel system, thereby leading to the increased stability observed for the antimicrobial SSDZ-loaded hydrogels produced.

Mathematical modelling of SSDZ release pattern from the hydrogel

In order to ascertain whether storage exerted a deleterious effect on SSDZ release from the hydrogel, samples from the stored SSDZ-loaded hydrogel were immersed in a low volume of ultrapure water, under dynamic flow conditions. The silver content in the solution was determined by potentiometry to study the SSDZ release behavior from the hydrogel. The potentiometric determinations showed that the silver release profile changed little as a function of storage time and that release was higher for prolonged storage times. Initially, and up to 30 min, there was a continued release of SSDZ, suggesting that SSDZ release took place through swelling of the hydrogel. Within ca. 10 to 15 min of immersion in solvent, a linear increase in the silver content in the diluent medium was observed. After this period, the concentration of silver in the solution continued to increase steadily, indicating a probable degradation of the hydrogel
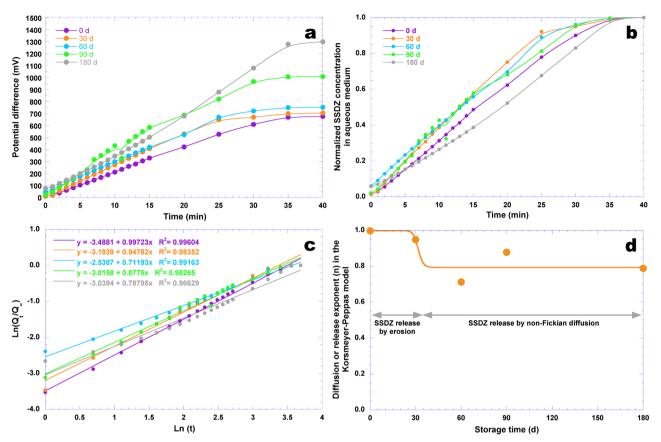
structure. To shed light on the release profile of silver sulfadiazine (SSDZ) from the hydrogel, and because after 35 min the amount of SSDZ released reached a plateau during the assay timeframe, the mathematical models were applied to the drug release data from the SSDZ-loaded hydrogels during storage time. The SSDZ release from the hydrogel did not occur by diffusion but by the erosion of the polymeric matrix. The fitting performed shows a poorer r^2 for both first-order and Higuchi models and an almost perfect r^2 for the Korsmeyer-Peppas model. This is in fact supported by the model fittings performed to the experimental SSDZ release data, which produced a correlation coefficient (r^2) (Table IV).

TABLE IV - Mathematical models applied to data for the experimental SSDZ hydrogel release

Time (d)	First-order model r^2	Higuchi model r^2	Korsmeyer-Peppas model r^2
0	0.69959	0.84236	0.99604
30	0.62130	0.88794	0.98352
60	0.76640	0.91610	0.99163
90	0.65341	0.89886	0.98265
180	0.88636	0.80012	0.96629

r^2 = correlation coefficient

The fitting performed shows a poorer r^2 for both first-order and Higuchi models and an almost perfect r^2 for the Korsmeyer-Peppas model. Additionally, the diffusion or release exponent (n) in the Korsmeyer-Peppas model produced by fitting the model to the SSDZ release data was n=0.9972 (0 d), n=0.9478 (30 d), n=0.7119 (60 d), n=0.8775 (90 d) and n=0.7879 (180 d) (in Korsmeyer-Peppas drug release model, n=0.45 suggests Fickian diffusion, 0.45<n<0.89 suggests anomalous diffusion or non-Fickian diffusion, and n≥0.89 suggests erosion of the polymeric chain), which indicates that SSDZ release from the SSDZ-loaded hydrogels occurred initially and up to 30 d of storage by erosion of the hydrogel's polymeric chain. After the first month of storage, the SSDZ release from the hydrogel occurred by anomalous diffusion or non-Fickian diffusion. The release results (in the form of potential differences (Figure 9a) and normalized SSDZ concentration in the aqueous medium (Figure 9b) have thus indicated continuous release during the timeframe assayed within the first 35 min of immersion of the hydrogel in a low-volume aqueous medium. The silver sulfadiazine concentration maintained a plateau, thereafter, thus confirming that complete erosion of the polymeric matrix occurred.
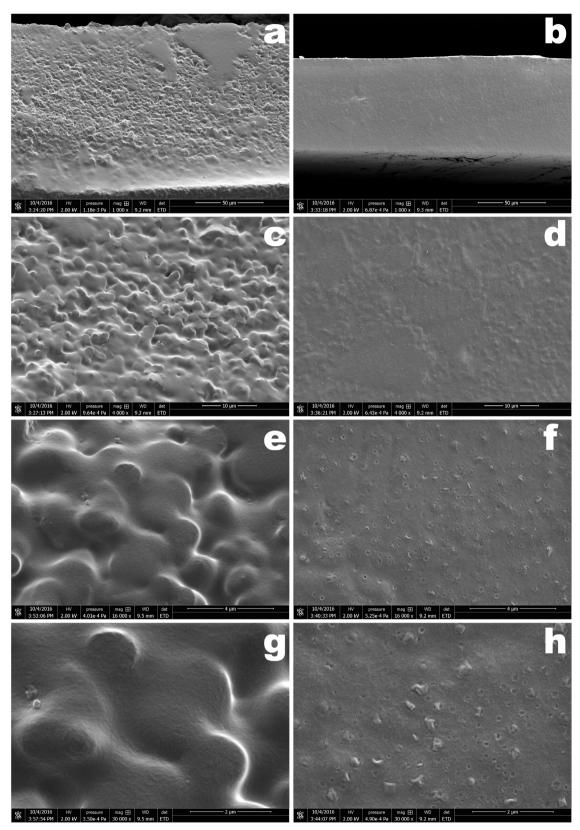
FIGURE 9 - Mathematical modelling of the SSDZ release assays for SSDZ-loaded hydrogels. Potential difference of the aqueous solution with samples of SSDZ-loaded hydrogels (a); normalized silver sulfadiazine concentration released (b). Linear fitting performed for transformed experimental data, using Korsmeyer- Peppas model (c); diffusion or release exponent (n) in Korsmeyer-Peppas model as a function of SSDZloaded hydrogel storage time reveals change in SSDZ release pattern (d).

The linear fitting performed for the transformed SSDZ release data using the Korsmeyer-Peppas model (Figure 9c) revealed a near perfect fit, further supporting the conclusion that SSDZ release from the SSDZ-loaded hydrogels occurred initially and up to 30 d of storage by erosion of the hydrogel's polymeric chain, whereas after the first month of storage the SSDZ release from the hydrogel occurred by anomalous diffusion or non-Fickian diffusion (Figure 9d). Although the slower release is intended for real skin wound applications, it should be noted that the experimental setup involved complete immersion of the hydrogel under dynamic flow conditions. In a real situation where the hydrogel is intended for application to a skin wound, the exudation produced should be static and not as abundant, and thus

the erosion of the hydrogel with concomitant release of SSDZ should be much slower.

Structural microanalysis of the SSDZ-loaded hydrogels by FESEM

The results observed in Figure 10 indicate a uniform morphology for the SSDZ-loaded hydrogels. with points of deposition of silver sulfadiazine. The prolonged storage rendered the hydrogel more brittle, with a marked difference in the fracture patterns of SSDZ-loaded hydrogels at time zero (Figures 10a (x1000), 10c (x4000), 10e (x16000), 10g (x30000)) and time 180 days (Figures 10b (x1000), 10d (x4000), 10f (x16000), 10h (x30000)).

FIGURE 10 - Scanning electron photomicrographs of SSDZ-loaded hydrogels at beginning (a: x1000; c: x4000; e: x16000; g: x30000) and end of180 d storage timeframe (b: x1000; d: x4000; f: x16000; h: x30000).

The polymeric structures exhibited by the SSDZ-loaded hydrogel formulation facilitate solvation and dissolution upon contact with the solvent, skin moisture and skin burns, providing a slow release of silver sulfadiazine content. The hydrogel micrographs in Figure 10 show that the hydrogel topography is highly uniform, irrespective of the storage timeframe.

CONCLUSIONS

The SSDZ-loaded hydrogels developed did not exhibit potential for cytotoxicity, and so they can be utilized in occlusive wound dressings. All hydrogels presented, after 48 hours of contact, results of cytotoxicity lower than 70% which, according to ISO 10993, indicates that they are not toxic to the cells. The hydrogels developed may be considered as a non-adherent dressing able to maintain a moist gel layer over the wound and are not expected to adhere to the wound or bandage, provided that it is not allowed to dry out. The SSDZ-loaded hydrogels had good characteristics in relation to immediate and continued release of the active antimicrobial principle over time, although different release processes of SSDZ occurred during the storage timeframe. The release of SSDZ occurred by the erosion of the hydrogel's polymeric chain during the first 30 d of storage and by non-Fickian diffusion for prolonged storage times. Although the release mechanism changed over storage time, the antimicrobial capability of the films was maintained. Additionally, the SSDZ-loaded hydrogels suffered some visual and physical changes along storage timeframe, such as darkening, as well as some changes in mechanical resistance, a decrease of crystallinity and narrowing of the melting profile. However, these changes did not compromise either its use as occlusive wound dressings or its antimicrobial properties.

ACKNOWLEDGEMENTS

REFERENCES

Ahmed EM. Hydrogel: preparation, characterization, and applications. J Adv Res. 2015;6:105-121.

Asadinezhad A, Lehocký M, Sáha P, Mozetic M. Recent progress in surface modification of polyvinyl chloride. Materials. 2012;5(12):2937-2959.

Bagul U, Sivakumar, SM. Antibiotic susceptibility testing: a review on current practices. Int J Pharm. 2016;6(3):11-17.

Bajaj S, Singla D, Sakhuja N. Stability testing of pharmaceutical products. J App Pharm Sci. 2012;2(3):129-38.

Baker MI, Walsh SP, Schwartz Z, Boyan BD. A review of polyvinyl alcohol and its uses in cartilage and orthopedic applications. J Biomater Mater Res B: App Biomater. 2012;100(5):1451-1457.

Balcão VM, Mateo C, Fernández-Lafuente R, Malcata FX, Guisán JM. Structural and functional stabilization of L-asparaginase via multi-subunit immobilization onto highly activated supports. Biotechnol Prog. 2001a;17(3):537-42.

Balcão VM, Mateo C, Fernández-Lafuente R, Malcata FX, Guisán J M. Coimmobilization of L-asparaginase and glutamate dehydrogenase onto highly activated supports. Enzyme Microb Technol. 2001b;28(7):696-704.

Bhagyashree P, Karishma G, Sampada A, Ankita P, Pratibha C, Kailash V. Recent trends in stability testing of pharmaceutical products: a review. Res J Pharm Biol Chem Sci. 2015;6(1):1557-1569.

Boutrand J. (ed.) Biocampatibility and performance of medical devices. Philadelphia: Woodhead Publishing; 2012.

Chirani N, Yahia L, Gritsch L, Motta F, Chirani S, Faré S. History and applications of hydrogels. J Biomed Sci. 2015;4(2):13-23.

CLSI. Performance Standards for Antimicrobial Susceptibility Testing: Twenty-First Informational Supplement. CLSI document M100-S21. Wayne, PA: Clinical and Laboratory Standards Institute, 2011.

Farjado R, Lopes LC, Caleare AO, Britta EA, Nakamura CV, Rubira AF, et al. Silver sulfadiazine loaded chitosan/chondroitin sulfate films for a potential wound dressing application. Mater Sci Eng Mater C. 2013;33(2):588-595.

Ganji F, Vasheghani-Farahani S,Vasheghani-Farahani E. Theoretical description of hydrogel swelling: a review. Irian Polymer J. 2010;19(5):375-398.

Giannelli M, Chellini F, Margheri M, Toneli P, Tani A. Effect of chlorhexidine digluconate on different cell types: a molecular and ultrastructural investigation. Toxicol in Vitro. 2008;22(2):308-17.

Guo J, Shalav E, Smith S. Physical stability of pharmaceutical formulations: solid-state characterization of amorphous dispersions. Trends Anal Chem. 2013;49:137-44.

Hiro ME, Pierpont YN, Ko F, Wright TE, Robson MC, Payne WG. Comparative Evaluation of silver-containing antimicrobial dressings on in vitro and in vivo processes of wound healing. Eplasty. 2012;12:e48. Available from: https://www.ncbi.nlm.nih.gov/pmc/articles/PMC3471607/

Hora DKOB, Taets DCGG, de Castro JO, Chico MR, Henrique MD. Brazilian recommendations for handling of the current coverings in the treatment of the burned patient. J Nurs Patient Care. 2017;2(2):1-5.

International Consensus. Appropriate use of silver dressings in wounds. An expert working group consensus. London: Wounds International, 2012. http://www.woundsinternational.com/media/issues/567/files/content_10381.pdf Accessd 9 fev 2017.

ISO. International Organization for Standardization. Biological evaluation of medical devices. Part 5: Tests for in vitro cytotoxicity ISO 10993-5, 3th ed., Switzerland, 2009.

Jodar KRS, Balcão VM, Chaud MV, Matthieu T, Yoshida VMH, Oliveira Jr JM, et al. Development and characterization of a hydrogel containing silver sulfadiazine for antimicrobial topical applications. J Pharm Sci. 2015;104(7):2241-54.

Kiviranta L, Kumpulainen S. Quality Control and Characterization of Bentonite Materials. Working Report. 2011-84, 2011.

Lamas EM, Barros RM, Balcão VM, Malcata FX. Hydrolysis of whey proteins by proteases extracted from *Cynara cardunculus* and immobilized onto highly activated supports. Enzyme Microb Technol. 2001;28(7-8):642-652.

Lansdown ABG. A pharmacological and toxicological profile of silver as an antimicrobial agent in medical devices. Adv Pharm Sci. 2010;2010:1-16.

Lansdown ABG. Silver in health care: antimicrobial effects and safety in use. Curr Probl Dermatol. 2006;33:17-34.

Madaghiele M, Demitri C, Sannino A, Ambrosio L. Polymeric hydrogels for burn wound care: Advanced skin wound dressings and regenerative templates. Burns Trauma. 2014;2(4):153-161.

Matty FS, Sultan MT, Amine AK. Swelling behavior of cross-link PVA with glutaraldehyde. Ibn Al-Haitham J Pure App Sci. 2015;28(2):136-46.

McShan D, Ray PC, Yu H. Toxicity mechanism of nanosilver. J Food Drug Anal. 2014;22(1):116–27.

Mehta P, Sharma D, Dashora A, Sahu D, Garg RK, Agrawal P, et al. Design, development and evaluation of lipid based topical formulations of silver sulfadiazine for treatment of burns and wounds. Innovare J Life Sci. 2013;1(1):38- 44.

Meva FE, Segnou ML, Ebongue CO, Ntoumba AA, Kedi PBE, Deli V, et al. Spectroscopic synthetic optimizations monitoring of silver nanoparticles formation from *Megaphrynium macrostachyum* leaf extract. Braz J Pharmacogn. 2016;26(2):640-646.

Migneault I, Dartiguenave C, Bertrand MJ, Waldron KC. Glutaraldehyde: behavior in aqueous solution, reaction with proteins, and application to enzyme crosslinking. BioTechniques 2004;37(5):790-802.

Moser H, Pereima RR, Pereima MJL. Evolution of silver dressings in the treatment of partial thickness burns. Rev Bras Queimaduras. 2013;12(2):60-67.

Munteanu A, Florescu IP, Niteseu C. A modern method of treatment: The role of silver dressings in promoting healing and preventing pathological scarring in patients with burn wounds. J Med Life. 2016;9(3):306-315.

Murphy DJ, Sankalia MG, Loughlin RG, Donnelly RF, Jenkins MG, McCarron PA. Physical characterisation and component release of poly(vinyl alcohol)-tetrahydroxyborate hydrogels and their applicability as potential topical drug delivery systems. Inter J Pharm. 2012;423(2):326-34.

Parparita E, Cheaburu CN, Patachia SF, Vasile C. Polyvinyl alcohol/chitosan/montmorillonite nanocomposites preparation by freeze/thaw cycles and characterization. Acta Chem IASI. 2014;22(2):75-96.

Peppas NA, Merrill EW. Differential scanning calorimetry of crystallized PVA hydrogels. J App Polym Sci. 1976;20(6):1457-65.

Petkovsek A, Macek M, Majes B. A laboratory characterization of soils and clay-bearing rocks using the Enslin-Neff water-adsorption test. Acta Geotech Slov. 2009;2:5-13.

Reis EF, Campos FS, Lage AP, Leite RC, Heneine LG, Vasconcelos WL, et al. Synthesis and characterization of poly (vinyl alcohol) hydrogels and hybrids for rMPB70 protein adsorption. Mater Res. 2006;9(2):185-91.

Rigo C, Ferroni L, Tocco I, Roman M, Munivrana I, Gardin C, et al. Active silver nanoparticles for wound healing. Int J Mol Sci. 2013;14(3):4817-40.

Sadahira CM, Souza AN, Mansur HS. Characterization of poly (vinyl alcohol) hydrogels crosslinked by Chemical Method and γ-Radiation. 9º Brazilian Congress of Polymers, 2007.

Schmidt U, Jorsch C, Guenther M, Gerlach G. Biochemical piezoresistive sensors based on hydrogels for biotechnology and medical applications. J Sens Sens Syst. 2016;5:409-417.

Shahzad MN, Ahmed N. Effectiveness of *Aloe Vera* gel compared with 1% silver sulphadiazine cream as burn wound dressing in second degree burns. J Pak Med Assoc. 2013;63(2):225-30.

Sepantafar M, Maheronnaghsh R, Mohammadi H, Radmanesh F, Hebrahimi M, Hasani-sadrabad MM, et al. Engineered hydrogels in cancer therapy and diagnosis. Trends Biotechnol. 2017;35(11):1074-1087.

Serra R, Grande R, Butrico L, Rossi A, Settimio UF, Caroleo B, et al. Chronic wound infections: the role of *Pseudomonas aeruginosa* and *Staphylococcus aureus*. Expert Rev Anti Infect Ther. 2015; 13(5):605-13.

Song A, Rane AA, Christman KL. Antibacterial and cell-adhesive polypeptide and poly(ethylene glycol) hydrogel as a potential scaffold for wound healing. Acta Biomater. 2012;8(1):41-50.

Ullah F, Othman MBH, Javed F, Ahmad Z, Akil H. Md. Classification, processing and application of hydrogels: A review. Mater Sci Eng C. 2015;57:414-433.

Vashist A, Vashist A, Gupta YK, Ahmad S. Recent advances in hydrogel based drug delivery systems for the human body. J Mater Chem B. 2014;(2):147-66.

Vila MMDC, Coelho SL, Chaud MV, Tubino M, Oliveira Jr JM, Balcão V M. Development and characterization of a hydrogel containing nitrofurazone for antimicrobial topical applications. Curr Pharm Biotechnol. 2014;15(2):182-90.

Yang T. Mechanical and swelling properties of hydrogels, KTH Ytbehandlingsteknik, Doctoral thesis, 2012, p. 77. http://www.diva-portal.org/smash/get/diva2:571374/FULLTEXT01.pdf.

Yu F, Cao X, Du J, Wang G, Chen X. Multifunctional hydrogel with good structure integrity, self-healing, and tissue-adhesive property formed by combining diels-alder click reaction and acylhydrazone bond. ACS Appl Mater Interfaces 2015;7(43):24023−24031.

Zhang T, Wang L, Chen Q, Chen C. Cytotoxic potential of silver nanoparticles. Yonsei Med J. 2014;55(2)283-291.